

ADAPTIVE WAVEFORM DESIGN FOR AUTOMOTIVE JOINT RADAR-COMMUNICATIONS SYSTEM

S. Hossein Dokhanchi[†], M. R. Bhavani Shankar[†], M. Alaei-Kerahroodi[†], T. Stifter[‡], and Björn Ottersten[†]

SnT, University of Luxembourg.[†], IEE S.A., Luxembourg [‡]

ABSTRACT

Single waveform design for automotive joint radar-communications (JRC) is being increasingly considered of late. This paper formulates the JRC design as an optimization problem exploiting the co-location of the two systems and investigates the trade-off between them. We propose an algorithm to maximize the performance of communication and radar receivers (e.g., BER and probability of detection, respectively). This intractable optimization problem is decomposed into two subproblems, which are subsequently solved in succession through a combination of gradient projection method and convex relaxations. The benefits of the proposed waveform are illustrated through numerical simulations.

Index Terms— Joint automotive radar-communications, waveform design, radar-communications trade-off.

1. INTRODUCTION

Intelligent transportation systems (ITS), such as emerging autonomous vehicles, aim at low-cost, compact and efficient sensing and communication devices by combining common resources of different sensors in a single system [1, 2]. Such a system, referred to as joint radar-communications (JRC), enables the sensing and communication systems to share spectrum for operations and hardware resources. Further, a JRC system benefits from mutual sharing of information between the systems, enabling hybrid processing to further enhance automotive safety and comfort. Realizing the importance of JRC, recent works [3–5], have investigated various ways for multiplexing radar and communications in different dimensions, i.e., code, space, time and frequency, when there is no prior knowledge about the target scene. In addition to the aforementioned investigations, several works have considered optimization of the waveform in different scenarios towards enhancing the identified radar tasks and communication performance [6–8]. Central to these works is the apriori knowledge on clutter/channel state information (CSI). It should be noted that the JRC landscape is rich in scenarios depending on the nature of sensing and communications, e.g., Bistatic

sensing [3–5], detection enhancement [8] etc. Performance analysis of such systems, central to their feasibility and implementation, has been undertaken in [9], [10], [11].

Our work focuses on JRC waveform optimization in a scenario where a JRC equipped automobile needs to communicate interactively with a similarly equipped terminal while also sensing passive targets, i.e., pedestrians, bicycles, in the latter’s vicinity. The novelty of the scenario, as opposed to two individual systems, lies in the exploitation of the bidirectional communication link in enhancing radar task. In particular, the communication link enables acquisition of partial CSI which can be further exploited. In this context, the JRC waveform is designed to optimize signal-to-noise-ratio (SNR) at the communication receiver (denoted as SNR_c as well as the signal-to-noise-plus-clutter-ratio (SNCR) of backscatter from passive targets simultaneously. Towards this, we follow a two step procedure of deriving optimal sequences to maximize SNR_c first followed by its perturbation to satisfy the desired SNCR; the perturbation level is a design parameter enabling trade-off between the two functionalities.

In contrast to the most conventional single JRC waveform designs that optimize an unified objective function for both radar and communications [12], we define separate objective functions for the two systems, but connect them through a similarity trade-off constraint. The advantage of this approach is ease of separating the optimization problem into two subproblems which are connected through a trade-off constraint. A work similar to this paper is [13], where downlink multiuser interference is minimized by enforcing both constant modulus and similarity constraints with respect to referenced radar signals. However, they do not consider Doppler shifts in their calculations, thereby limiting the scope of its application. On the contrary, in this work, SNCR is maximized based on worst case Doppler scenario. Another contribution of the work is the inclusion of integrated side-lobe level (ISL) constraint of the designed sequences in order to leverage the high resolution property of the MIMO systems [14].

Notation: Bold lowercase and uppercase denote vectors and matrices, respectively. $(\cdot)^T$ and $(\cdot)^H$ denote the transpose and Hermitian operators, respectively. \mathbf{I}_n represents $n \times n$ identity matrix, $[c_{i,j}]_{i=1,j=1}^{N,M}$ denotes a $N \times M$ matrix, $\|\mathbf{C}\|_F$ stands for Frobenius norm, $\text{Diag}\{\mathbf{c}\}$ denotes a matrix with elements of vector \mathbf{c} on its diagonal, inner product between

This work is supported by the Luxembourg National Research Fund under grants Ref. 11638687 (AFR-PPP).

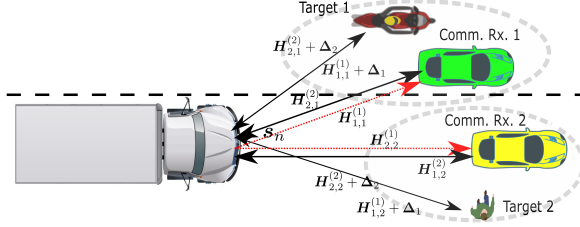


Fig. 1. JRC scenario: Truck distributes messages to communication receivers and performs detection and ranging of 'Target 1' and 'Target 2' simultaneously through the same transmit signal s_n ; $\mathbf{H}_{n,q}^{(1)}$, $\mathbf{H}_{q,n}^{(2)}$ comprise CSI for JRC links.

two matrices represented by $\mathbf{X} \bullet \mathbf{Y} = \Re\{\text{tr}\{\mathbf{X}^H \mathbf{Y}\}\}$ where 'tr' denotes the trace of a matrix. The notation $\mathbf{X} \succeq 0$ means \mathbf{X} is a positive semidefinite matrix. E denotes Expectation.

2. SIGNAL AND SYSTEM MODEL

Fig. 1 shows the scenario where the JRC transmitter (truck) transmits a set of modulated sequences from N antennas to sense the targets e.g., bike, pedestrian. This sequence also conveys a communication symbol to the JRC receivers, e.g. two cars. Without loss of generality, we assume one target in the vicinity of each JRC receiver. Let $s_n(l)$ be a L length sequence and a_n be the communication symbols on n th antenna with $n \in [1, N]$. The sampled transmit signal takes the form, $\tilde{s}_n(l) = a_n s_n(l)$, $l \in [1, L]$ during the transmission time T . In this work, we are interested in the design of $s_n(l)$, $\forall n, l$ while a_n can be drawn from any modulation. Towards this, let $\mathbf{s}_n = [s_n(l)]_{l=1}^L \in \mathbb{C}^L$, and define $\mathbf{s} = [\mathbf{s}_n]_{n=1}^N \in \mathbb{C}^{LN}$.

2.1. Signal model at JRC receiver

Let $\mathbf{h}_{qn} = [h_{qn}(i)]_{i=1}^{\tilde{L}}$ be a wide-sense-stationary Gaussian process [8], containing \tilde{L} arbitrary clutter/CSI components along the path from transmit antenna n to the JRC receiver q . With superscript (1) indicating CSI from transmitter and $\mathbf{H}_{qn}^{(1)}$ to be the convolution matrix generated from \mathbf{h}_{qn} , the discrete convolution between the radar waveform \mathbf{s}_n and \mathbf{h}_{qn} takes the form, [15]

$$\mathbf{H}_{qn}^{(1)} = \begin{bmatrix} h_{qn}(1) & 0 & \dots & \dots & \dots & 0 \\ h_{qn}(2) & h_{qn}(1) & 0 & \dots & \dots & 0 \\ \vdots & \vdots & \ddots & \vdots & \vdots & \vdots \\ 0 & \dots & 0 & h_{qn}(\tilde{L}) & \dots & h_{qn}(1) \end{bmatrix} \in \mathbb{C}^{L \times L}.$$

Let the Doppler vector for q th JRC link be $\mathbf{e}_q = [e^{-j2\pi f_{D_q} l t_s}]_{l=0}^L$ where f_{D_q} denotes the corresponding Doppler shift. We collect the Doppler shifts between all JRC receivers and the transmitter (cars and the truck in Fig. 1) over the period of transmission into $\mathbf{E}_1 = \text{Diag}\{[\mathbf{e}_q]_{q=1}^Q\} \in \mathbb{C}^{M_1 \times M_1}$. Similarly, let $\mathbf{H}_1 = [\mathbf{H}_{qn}^{(1)}]_{q=1, n=1}^{Q, N} \in \mathbb{C}^{M_1 \times M_2}$ models all paths from transmit to JRC receivers, where $M_1 = LQ$, $M_2 = LN$

. We stack the received signal at all JRC receivers as,

$$\mathbf{y} = \mathbf{E}_1 \mathbf{H}_1 \mathbf{s} + \mathbf{n}_1 \in \mathbb{C}^{M_1}, \quad M_1 = LQ \quad (1)$$

where \mathbf{n}_1 is the zero-mean complex-valued circular Gaussian noise with known covariance matrix at the receivers of all communicating vehicles.

We further define \mathbf{H}_2 similar to \mathbf{H}_1 to model the channel presented by

$$\mathbf{H}_2 = [\mathbf{H}_{nq}^{(2)}]_{n=1, q=1}^{N, Q} \in \mathbb{C}^{M_2 \times M_1}, \quad M_2 = NL \quad (2)$$

where $\mathbf{H}_{nq}^{(2)}$ is similar to $\mathbf{H}_{nq}^{(1)}$ models the elements between JRC vehicle q and n th antenna of the truck.

2.2. Signal model at radar receiver on the truck

Similar to \mathbf{E}_1 , let $\mathbf{E} \in \mathbb{C}^{M_1 \times M_1}$ collect the Doppler shifts from the backscatter of all the passive targets (pedestrian and cyclist in Fig. 1) on its diagonal elements. Let matrix \mathbf{G} present the clutter (any signal dependent interference). Under the assumption of one passive target near each JRC receiver, the backscatters from the targets corresponding to the range-angle cell under examination can be written as

$$\mathbf{r} = (\mathbf{H}_2 + \mathbf{\Delta}_2) \mathbf{E} (\mathbf{H}_1 + \mathbf{\Delta}_1) \mathbf{s} + \mathbf{G} \mathbf{s} + \mathbf{n}_2 \in \mathbb{C}^{M_2}, \quad (3)$$

where $\mathbf{\Delta}_2 \in \mathbb{C}^{M_2 \times M_1}$ and $\mathbf{\Delta}_1 \in \mathbb{C}^{M_1 \times M_2}$ are Gaussian random variables with zero means and known variances to model uncertainty of the receive and transmit CSI of objects close to the active communicating vehicles, respectively. Further, \mathbf{n}_2 is the zero-mean complex-valued circular Gaussian noise with known covariance matrix at the radar receiver.

3. WAVEFORM DESIGN AND JRC ALGORITHM

In this section, we present a novel JRC waveform design algorithm to enhance performance for both radar and communications. The communication SNR, i.e., $\text{SNR}_c = \frac{\|\mathbf{y}\|^2}{E(\|\mathbf{n}_1\|^2)}$ obtained using (1) and radar SNCR obtained using (3), i.e., $\text{SNCR} = \frac{E\{\|(\mathbf{H}_2 + \mathbf{\Delta}_2) \mathbf{E} (\mathbf{H}_1 + \mathbf{\Delta}_1) \mathbf{s}\|^2\}}{E\{\|\mathbf{G} \mathbf{s}\|^2 + \|\mathbf{n}_2\|^2\}}$ are used as performance metrics. Clearly, appropriate CSI is needed for effecting the optimization, which is not typically available a priori in a radar system. The salient feature of JRC is now exploited to overcome this shortcoming.

The transmit and receive CSI, i.e., \mathbf{H}_1 and \mathbf{H}_2 , are estimated on the JRC link through pilot sequences. In particular, they are acquired during the establishment of a JRC link by sending and receiving known sequences and sharing the channel information among active communicating vehicles, through a small dedicated portion of the bandwidth. In addition, CSI is assumed to remain unchanged during one communication frame/radar pulse. This CSI, albeit partial for the radar system, can nevertheless be exploited.

3.1. Optimization problem for Communications

Towards maximizing SNR_c , it suffices to solve an optimization problem to maximize the received signal power $\|\mathbf{y}\|^2$. In addition, we impose additional constraints on integrated-sidelobe-level (ISL) of the designed sequences to enable radar tasks. Towards this, let $r_{kp}(l) = \sum_{n=1}^{L-l} \mathbf{s}_k(n)\mathbf{s}_p^*(n+l)$ denote the cross-correlation between the set of sequences, where $1 \leq k, p \leq N$, $-L+1 \leq l \leq L-1$, and $r_{kp}(l) = [r_{kp}(-l)]^*$. We define ISL of a set of N sequences, each of length L as

$$\text{ISL} = \sum_{k=1}^N \sum_{\substack{l=-L+1 \\ l \neq 0}}^{L-1} |r_{kk}(l)|^2 + \sum_{k=1}^N \sum_{\substack{p=1 \\ p \neq k}}^N \sum_{l=-L+1}^{L-1} |r_{kp}(l)|^2. \quad (4)$$

We define ISL in matrix form based on (4) as

$$\|\mathbf{s}\mathbf{s}^H - \text{Diag}\{\mathbf{s}\mathbf{s}^H\}\|_F^2 \quad (5)$$

Without loss of generality, we consider unit power transmission and formulate the SNR_c optimization problem as

$$P_1^{\text{Comm.}} \begin{cases} \max_{\mathbf{s}} & \|\mathbf{E}_1 \mathbf{H}_1 \mathbf{s}\|^2 \\ \text{subject to} & \mathbf{c}_1 : \|\mathbf{s}\|^2 = 1, \quad \text{power constraint} \\ & \mathbf{c}_0 : \|\mathbf{s}\mathbf{s}^H - \text{Diag}\{\mathbf{s}\mathbf{s}^H\}\|_F^2. \end{cases}$$

Since $\mathbf{E}_1^H \mathbf{E}_1 = \mathbf{I}_{M_1}$, we can simplify $\|\mathbf{E}_1 \mathbf{H}_1 \mathbf{s}\|^2 = \mathbf{R}_{H_1}^H \bullet \mathbf{S}$ where $\mathbf{R}_{H_1} = [\mathbf{H}_1]^H \mathbf{H}_1$ and $\mathbf{S} = \mathbf{s}\mathbf{s}^H$. Using this, $P_1^{\text{Comm.}}$ reduces to,

$$P_2^{\text{Comm.}} \begin{cases} \max_{\mathbf{S}} & \mathbf{R}_{H_1}^H \bullet \mathbf{S} \\ \text{subject to} & \tilde{\mathbf{c}}_0 : \|\mathbf{S} - \text{Diag}\{\mathbf{S}^H\}\|_F^2 \leq \gamma, \\ & \mathbf{c}_2 : \text{rank}(\mathbf{S}) = 1, \\ & \mathbf{c}_3 : \mathbf{S} \succeq 0, \\ & \tilde{\mathbf{c}}_1 : \text{tr}\{\mathbf{S}\} = 1. \end{cases}$$

In order to solve $P_2^{\text{Comm.}}$ in polynomial-time, it is required to further relax it by removing the unity rank on \mathbf{S} as

$$P_3^{\text{Comm.}} \begin{cases} \max_{\mathbf{S}} & \mathbf{R}_{H_1}^H \bullet \mathbf{S} \\ \text{subject to} & \tilde{\mathbf{c}}_0, \tilde{\mathbf{c}}_1, \mathbf{c}_3. \end{cases}$$

Problem $P_3^{\text{Comm.}}$ can be solved by CVX [16] and we denote its optimal solution by \mathbf{c} . It is worthy to note that by dropping ISL condition, the maximum SNR value of the above objective function becomes $\max_{\mathbf{s}} \|\mathbf{H}_1 \mathbf{s}\|^2 = \lambda_{\max}\{\mathbf{R}_{H_1}\}$ which is an upper bound for solution to $P_3^{\text{Comm.}}$. Let the resulting sequence be denoted as \mathbf{c} .

3.2. Joint optimization problem

Having obtained the optimal communication waveform, \mathbf{c} , we proceed to the maximize SCNR_c . To enable this step while exploiting \mathbf{c} , we consider the following problem,

$$P_1^{\text{JRC}} \begin{cases} \max_{\mathbf{s}} \min_{f_D} & \frac{E\{[(\mathbf{H}_2 + \Delta_2)\mathbf{E}(\mathbf{H}_1 + \Delta_1)\mathbf{s}]^2\}}{E\{\|\mathbf{G}\mathbf{s}\|^2 + \|\mathbf{n}_2\|^2\}} \\ \text{subject to} & \mathbf{c}_4 : f_D \in \Omega^Q, \quad \text{Doppler region} \\ & \mathbf{c}_5 : \|\mathbf{s} - \mathbf{c}\|^2 \leq \delta, \quad \text{trade-off constraint} \\ & \mathbf{c}_0, \mathbf{c}_1. \end{cases}$$

Here, we consider the worst case scenario by minimizing the objective function with regard to a feasible Doppler region, i.e., Ω . This arises since there is no knowledge about Doppler shifts at the transmitter of JRC-equipped vehicle i.e., the truck. Further, δ determines the trade-off between the communications and radar systems. A large δ offers more flexibility in JRC waveform design (away from communications waveform). In contrast, for a small δ , there is little freedom for designing radar waveform.

In Table 1, we propose 'JRC algorithm' to solve the above max-min problem detailed in the next section by breaking it down into separate maximization and minimization problem. This enables an efficient, yet effective, design methodology exploiting available information. For this purpose, we first solve the following minimization problem P_1^{Doppler} with $\mathbf{s} = \mathbf{c}$ to find f_D^* as

$$P_1^{\text{Doppler}} \begin{cases} \min_{f_D} & \frac{E\{[(\mathbf{H}_2 + \Delta_2)\mathbf{E}(\mathbf{H}_1 + \Delta_1)\mathbf{c}]^2\}}{E\{\|\mathbf{G}\mathbf{c}\|^2 + \|\mathbf{n}_2\|^2\}} \\ \text{subject to} & \mathbf{c}_4. \end{cases}$$

Then considering $\tilde{\mathbf{E}} = \mathbf{E}\{f_D^*\}$, we solve problem $P_1^{\text{seq.}}$ to obtain the best JRC sequence,

$$P_1^{\text{seq.}} \begin{cases} \max_{\mathbf{s}} & \frac{E\{[(\mathbf{H}_2 + \Delta_2)\tilde{\mathbf{E}}(\mathbf{H}_1 + \Delta_1)\mathbf{s}]^2\}}{E\{\|\mathbf{G}\mathbf{s}\|^2 + \|\mathbf{n}_2\|^2\}} \\ \text{subject to} & \mathbf{c}_0, \mathbf{c}_1, \mathbf{c}_5. \end{cases}$$

3.2.1. Solution to the minimization problem P_1^{Doppler}

Let $g = E\{[(\mathbf{H}_2 + \Delta_2)\mathbf{E}(\mathbf{H}_1 + \Delta_1)\mathbf{c}]^2\}$ be the hyper-dimensional surface that needs to be minimized with respect to Doppler shifts. We propose the gradient projection method (GPM) for the problem P_1^{Doppler} [17]. This involves computing the gradient of g with respect to \mathbf{s} and projecting it into the feasible region. However, the function g being a non-constant real-valued function on the complex domain, is not analytic, hence its classical complex derivatives does not exist [17]. To deal with this difficulty, however, *generalized complex derivatives* can be defined. Hence the linear approximation of real-valued function g at \mathbf{z}_0 becomes $g(\mathbf{z}) \approx g(\mathbf{z}_0) + \nabla_{\mathbf{z}}g(\mathbf{z}_0)(\tilde{\mathbf{z}} - \mathbf{z}_0) = g(\mathbf{z}_0) + 2\Re\left\{\frac{\partial g}{\partial \mathbf{z}}(\mathbf{z}_0)(\mathbf{z} - \mathbf{z}_0)\right\}$ where $\tilde{\mathbf{z}} - \mathbf{z}_0 = [\mathbf{z} - \mathbf{z}_0 \quad \mathbf{z}^* - \mathbf{z}_0^*]^T$ and $\nabla_{\mathbf{z}}g(\mathbf{z}_0) = \left[\frac{\partial g(\mathbf{z}_0)}{\partial \mathbf{z}} \quad \frac{\partial g(\mathbf{z}_0)}{\partial \mathbf{z}^*}\right]$.

The gradient of a scalar real-valued function $g(\mathbf{z})$ is therefore an augmented vector $\nabla_{\mathbf{z}}g(\mathbf{z}_0) = \left[\frac{\partial g(\mathbf{z}_0)}{\partial \mathbf{z}} \quad \left(\frac{\partial g(\mathbf{z}_0)}{\partial \mathbf{z}}\right)^*\right]$

where $\frac{\partial g}{\partial \mathbf{z}} = \left[\frac{\partial g}{\partial z_i}\right]_{i=1}^N$, $\frac{\partial g}{\partial \mathbf{z}^*} = \left[\frac{\partial g}{\partial z_i^*}\right]_{i=1}^N$. Therefore, we have $\frac{\partial g}{\partial f_{D_i}} = 2\Re\{\mathbf{c}^H \mathbf{H}_1^H \mathbf{E}^H \mathbf{H}_2^H \mathbf{H}_2 \frac{\partial \mathbf{E}}{\partial f_{D_i}} \mathbf{H}_1 \mathbf{c}\}$.

3.2.2. Solution to the problem $P_1^{\text{seq.}}$

We rewrite trade-off constraint of $P_1^{\text{seq.}}$ as $(\mathbf{s} - \mathbf{c})^H (\mathbf{s} - \mathbf{c}) = 2 - 2\Re(\mathbf{s}^H \mathbf{c}) \leq \delta$ using unity power constraint. We re-

Table 1. JRC algorithm

Step 1: Solve problem P_3^{Comm} to obtain optimal communications sequence \mathbf{c} .

Step 2: Fix sequence \mathbf{s} to optimal communications sequence \mathbf{c} and estimate \mathbf{f}_D by solving problem P_1^{Doppler} through gradient projection method as described in subsection 3.2.1.

Step 3: Using \mathbf{f}_D from Step 3 to obtain a solution $\tilde{\mathbf{S}}$ for the problem P_3^{seq} by CVX.

Step 4: Recovering vector \mathbf{s} from SVD decomposition of PSD matrix $\tilde{\mathbf{S}}$ using the tips at the end of section 3.2.2.

lax the trade-off constraint $\Re(\mathbf{s}^H \mathbf{c}) \geq \beta, \beta = (1 - \frac{\delta}{2})$ as $\text{tr}\{\mathbf{S}\mathbf{C}\} \geq \epsilon$ where $\mathbf{S} \succeq 0, \mathbf{C} = \mathbf{c}\mathbf{c}^H$ and ϵ is a threshold (please see [18] for more details). After some simplification, the numerator of the SNCR becomes

$$\mathbf{s}^H \left(\mathbf{H}_1^H \mathbf{E}^H \mathbf{R}_{H_2} \mathbf{E} \mathbf{H}_1 + M_2 \sigma^2 \mathbf{R}_{H_1} + \sigma^2 \text{tr}\{\mathbf{R}_{H_2}\} \mathbf{I}_{M_2} + M_1 M_2 \sigma^4 \mathbf{I}_{M_2} \right) \mathbf{s} = \mathbf{s}^H \mathbf{W} \mathbf{s} = \text{tr}\{\mathbf{W} \mathbf{s} \mathbf{s}^H\},$$

where $\mathbf{R}_{H_1} = \mathbf{H}_1^H \mathbf{H}_1 \in \mathbb{C}^{M_2 \times M_2}$ and $\mathbf{R}_{H_2} = \mathbf{H}_2^H \mathbf{H}_2 \in \mathbb{C}^{M_1 \times M_1}$ and the denominator becomes $\mathbf{s}^H \mathbf{R}_G \mathbf{s} + M_2 \sigma_{n_2}^2$. Normally an estimation of the covariance matrix of the clutters, i.e., $\hat{\mathbf{R}}_G$ is provided. Similar to P_2^{Comm} , we only consider the real part of the objective function, i.e., $\mathbf{W}^H \bullet \mathbf{S}$ and also removing the unity rank condition on \mathbf{S} . Thus we rewrite P_1^{seq} as

$$P_2^{\text{seq}} \begin{cases} \max_{\mathbf{S}} & \frac{\mathbf{W}^H \bullet \mathbf{S}}{\hat{\mathbf{R}}_G^H \bullet \mathbf{S} + M_2 \sigma_{n_2}^2} \\ \text{subject to} & \tilde{\mathbf{c}}_5 : \text{tr}\{\mathbf{S}\mathbf{C}\} = \epsilon, \tilde{\mathbf{c}}_0, \tilde{\mathbf{c}}_1, \mathbf{c}_3. \end{cases}$$

Linear fractional programs are addressed in [19] by variable transformation. To this end, we introduce a slack variable $\rho \geq 0$ where $\tilde{\mathbf{S}} = \rho \mathbf{S}$. We modify P_2^{seq} as the following optimization problem

$$P_3^{\text{seq}} \begin{cases} \max_{\mathbf{S}, \rho} & \mathbf{W}^H \bullet \tilde{\mathbf{S}} \\ \text{subject to} & \mathbf{R}_G^H \bullet \tilde{\mathbf{S}} + M_2 \sigma_{n_2}^2 \rho = 1 \\ & \text{tr}\{\tilde{\mathbf{S}}\mathbf{C}\} = \epsilon \rho, \text{tr}\{\tilde{\mathbf{S}}\} = \rho \\ & \tilde{\mathbf{S}} \succeq 0, \|\tilde{\mathbf{S}} - \text{Diag}\{\tilde{\mathbf{S}}\}\|_F^2 \leq \gamma \rho^2, \rho \geq 0. \end{cases}$$

Finding the solution \mathbf{S} for P_2^{seq} is straightforward using tools like CVX. We must then recover the transmit vector \mathbf{s} from positive semidefinite matrix \mathbf{S} . Based on Theorem 2.3. of [20], one can find a rank-one decomposition of a positive semidefinite matrix \mathbf{S} in polynomial-time. For decomposing \mathbf{S} into rank one approximation, one solution is to compute the SVD of the matrix \mathbf{S} and taking the singular-vector corresponding to the largest singular value.

4. NUMERICAL RESULTS

In this section, we present the performance comparison of various types of sequences and the optimal JRC sequence presented in Section 3. Fig. 2 shows receiver operating

characteristic (ROC) curves of optimal communications sequence, FFT sequence, a random sequence and our optimal JRC waveform at 8 dB SNCR for Neyman-Pearson detector. We observe that in case of optimal JRC waveform, the detection capability is enhanced significantly compared to other waveforms since it achieves a higher SNCR level at radar receiver for a given δ . Fig. 3 shows BER of communications

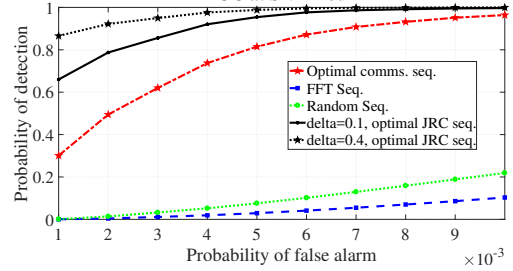


Fig. 2. Radar detection performance comparison for different types of sequences and optimal JRC sequence with similarity threshold level of ($\delta = 0.1, \delta = 0.4$), and ISL level of $\gamma = 0.8$.

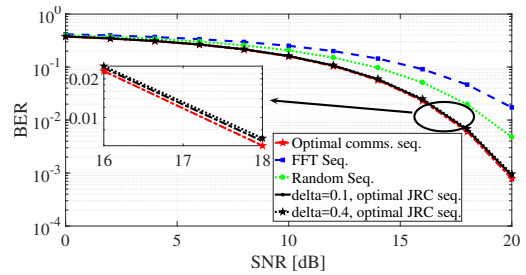


Fig. 3. Communications BER performance comparison for different types of sequences and optimal JRC sequence with similarity threshold level of ($\delta = 0.1, \delta = 0.4$), and ISL level of $\gamma = 0.8$.

for various sequences. We observe the optimal sequence for communications has the lowest BER. For small δ , BER of optimal JRC sequence is naturally close to optimal communication sequence BER. However, the radar performance is reduced and optimal communications waveform has the worst radar probability of detection among all type of sequences. By adjusting the trade-off factor δ one can find a waveform that satisfies a desired BER and P_d .

5. CONCLUSION

A new approach for single waveform design in automotive JRC is proposed to maximize simultaneously the SNR at the communication receiver as well as the SCNR at the radar receiver towards enhancing their respective performance. The design is formulated as an optimization problem and a simple methodology for obtaining a solution is proposed. The work highlights the benefits symbiotic existence of radar and communications benefits of JRC through CSI exchange and attaining optimal performance trade-offs.

6. REFERENCES

- [1] C. Sturm and W. Wiesbeck, "Waveform design and signal processing aspects for fusion of wireless communications and radar sensing," *Proceedings of the IEEE*, vol. 99, no. 7, pp. 1236–1259, 2011.
- [2] V. Winkler, J. Detlefsen, U. Siart, J. Buchler, and M. Wagner, "Automotive radar sensor with communication capability," in *European Conference on Wireless Technologies*, 2004, pp. 305–308.
- [3] S. H. Dokhanchi, M. R. Bhavani Shankar, Y. A. Nijssure, T. Stifter, S. Sedighi, and B. Ottersten, "Joint automotive radar-communications waveform design," in *IEEE International Symposium on Personal, Indoor and Mobile Radio Communications*, 2017.
- [4] S. H. Dokhanchi, M. R. B. Shankar, T. Stifter, and B. Ottersten, "OFDM-based automotive joint radar-communication system," in *2018 IEEE Radar Conference (RadarConf18)*, April 2018, pp. 0902–0907.
- [5] —, "Multicarrier phase modulated continuous waveform for automotive joint radar-communication system," in *2018 IEEE 19th International Workshop on Signal Processing Advances in Wireless Communications (SPAWC)*, June 2018, pp. 1–5.
- [6] B. Li, A. P. Petropulu, and W. Trappe, "Optimum co-design for spectrum sharing between matrix completion based MIMO radars and a MIMO communication system," *IEEE Transactions on Signal Processing*, vol. 64, no. 17, pp. 4562–4575, 2016.
- [7] P. Kumari, J. Choi, N. Gonzalez-Prelcic, and R. W. Heath, "IEEE 802.11ad-based radar: An approach to joint vehicular communication-radar system," *IEEE Transactions on Vehicular Technology*, vol. 67, no. 4, pp. 3012–3027, April 2018.
- [8] M. Bica, K. Huang, V. Koivunen, and U. Mitra, "Mutual information based radar waveform design for joint radar and cellular communication systems," in *2016 IEEE International Conference on Acoustics, Speech and Signal Processing (ICASSP)*, March 2016, pp. 3671–3675.
- [9] A. R. Chiriyath, B. Paul, and D. W. Bliss, "Simultaneous radar detection and communications performance with clutter mitigation," in *Radar Conference (RadarConf), 2017 IEEE*, 2017, pp. 0279–0284.
- [10] —, "Radar-communications convergence: Coexistence, cooperation, and co-design," *IEEE Transactions on Cognitive Communications and Networking*, vol. 3, no. 1, pp. 1–12, 2017.
- [11] A. R. Chiriyath, B. Paul, G. M. Jacyna, and D. W. Bliss, "Inner bounds on performance of radar and communications co-existence," *IEEE Trans. Signal Processing*, vol. 64, no. 2, pp. 464–474, 2016.
- [12] Y. Liu, G. Liao, J. Xu, Z. Yang, and Y. Zhang, "Adaptive OFDM integrated radar and communications waveform design based on information theory," *IEEE Communications Letters*, vol. 21, no. 10, pp. 2174–2177, 2017.
- [13] F. Liu, L. Zhou, C. Masouros, A. Lit, W. Luo, and A. Petropulu, "Dual-functional cellular and radar transmission: Beyond coexistence," in *2018 IEEE 19th International Workshop on Signal Processing Advances in Wireless Communications (SPAWC)*, June 2018, pp. 1–5.
- [14] M. M. Naghsh, M. Modarres-Hashemi, M. A. Kerahroodi, and E. H. M. Alian, "An information theoretic approach to robust constrained code design for MIMO radars," *IEEE Transactions on Signal Processing*, vol. 65, no. 14, pp. 3647–3661, July 2017.
- [15] J. Metcalf, C. Sahin, S. Blunt, and M. Rangaswamy, "Analysis of symbol-design strategies for intrapulse radar-embedded communications," *IEEE Transactions on Aerospace and Electronic Systems*, vol. 51, no. 4, pp. 2914–2931, 2015.
- [16] M. Grant, S. Boyd, and Y. Ye, "CVX: Matlab software for disciplined convex programming," 2008.
- [17] P. J. Schreier and L. L. Scharf, *Statistical signal processing of complex-valued data: the theory of improper and noncircular signals*. Cambridge University Press, 2010.
- [18] A. D. Maio, S. D. Nicola, Y. Huang, S. Zhang, and A. Farina, "Code design to optimize radar detection performance under accuracy and similarity constraints," *IEEE Transactions on Signal Processing*, vol. 56, no. 11, pp. 5618–5629, Nov 2008.
- [19] A. Charnes and W. W. Cooper, "Programming with linear fractional functionals," *Naval Research Logistics Quarterly*, vol. 10, no. 1, pp. 273–274, 1963.
- [20] W. Ai, Y. Huang, and S. Zhang, "New results on hermitian matrix rank-one decomposition," *Mathematical programming*, vol. 128, no. 1-2, pp. 253–283, 2011.